SEISMIC BEHAVIOUR OF MULTI-ARCHED AND MULTI-VAULTED HISTORICAL MASONRY STRUCTURES

ELISA MONTIS[1], AMAL GERGES[1], SALVADOR IVORRA[2] & MARIA CRISTINA PORCU[1]
[1]University of Cagliari, Italy
[2]University of Alicante, Spain

ABSTRACT

Ancient masonry structures are often made of arches, vaults and domes. Many of such structures stand in earthquake-prone countries of the Mediterranean area (like Italy, Spain and Lebanon). During their long life they have experienced different levels of seismic actions, suffering from minor damages to partial or total collapse. Although being robust and stable under vertical loads, unreinforced masonry constructions are typically vulnerable to horizontal actions which may induce out-of-plane mechanisms and the development of plastic hinges in arches and vaults. To preserve the vast Mediterranean historical built heritage, an in-depth comprehension of the seismic behaviour of arched and vaulted masonry constructions is thus essential. With the aim of contributing to this matter, the paper referred to three noteworthy case studies: a middle-age Italian tower, an eighteenth-century multi-arched Spanish aqueduct and an eighteenth-century multi-vaulted Lebanese hammam. Three-dimensional models of the real structures, identified via experimental modal tests, were considered. The anisotropic and non-linear behaviour of masonry was accounted for by means of an elastic–plastic damage constitutive law. Dynamic non-linear analyses were carried out under spectrum-consistent earthquakes to predict the damage pattern of the three different structures. Two kinds of earthquakes (pulse-like and multi-peak) were considered, and different ratios between tensile and compression strength were considered. The comparison of the results gives some insights on the post-elastic seismic demand on masonry buildings with linear or curved shapes under different kinds of earthquakes and for lowering values of the strength ratio.

Keywords: historical masonry structures, multi-arched, multi-vaulted, seismic assessment, non-linear time-history seismic analyses.

1 INTRODUCTION

Most historical buildings in the Mediterranean area are masonry structures that range from simpler cantilever-beam-like shapes (bell/civic towers, minarets) to multi-arched (bridges, aqueducts) and multi-vaulted (churches, mosques, hammams) geometries. In the last decades, many studies delt with the seismic assessment of heritage masonry buildings, involving towers and chimneys [1]–[4], bridges [5], [6], churches [7] and hammams [8]. Different kinds of analyses (linear, pushover, non-linear dynamic) and different modelling approaches have been adopted in such studies. Seldom, however, the role of the structural typology, the kind of earthquake, and the parameters adopted in the non-linear constitutive law of masonry material have been investigated in a comparative study.

With reference to three noteworthy case studies, a comparative investigation was carried out on the post-elastic response of tower-like, in-plane multi-arched and spatial multi-vaulted historical masonry structures. The first case study was the L'Aquila civic tower (Italy), which is an example of the typical cantilever-beam behaviour of tower-like unreinforced masonry monuments. Reference to the study of the L'Aquila civic tower conducted in Porcu et al. [2] was made. The second case study was Los Cinco Ojos aqueduct (Spain) which is currently being studied by the authors. This is considered as a benchmark of the seismic behaviour of multi-arched masonry structures like bridges and monumental aqueducts. The third structure considered in the investigation was the Hammam of Beit-el-Din (Lebanon), a magnificent

WIT Transactions on The Built Environment, Vol 217, © 2025 WIT Press
www.witpress.com, ISSN 1743-3509 (on-line)
doi:10.2495/ERES250071

building made of pierced vaults and domes the seismic vulnerability of which was recently studied by Gerges et al. [8].

With the aim of assessing the role of the structural shape (with and without arches/vaults) and of the earthquake type (pulse-like or multi-peak), non-linear dynamic analyses under two earthquakes consistent with the Lebanese design response spectrum are carried out for the three case studies, by assuming a concrete damage plasticity constitutive law for masonry. The role of the strength ratio assumed in the constitutive model is also evaluated.

2 REFERENCE CASE STUDIES

To check the role of some parameters on the numerical response of multi-arched and multi-vaulted masonry structures and to compare the seismic demand on different structural geometries, three case studies are considered. They are briefly described in Sections 2.1, 2.2 and 2.3.

2.1 L'Aquila civic tower

The civic tower of L'Aquila (Fig. 1(a)) is a 39.50 m high masonry monument, built in Italy in the thirteenth century. It has an almost squared base section (6.26 m × 6.46 m) and tapered walls made of limestone blocks (Fig. 1(b)). The seismic behaviour of this structure was studied in Porcu et al. [2], where a three-dimensional (3D) finite element model (Fig. 1(c)) was developed with C3D10 elements in ABAQUS [9] and identified by comparison with experimental frequencies. The identified elastic parameters are provided in Table 1. Fixed base constraints were assumed and no interaction with the soil was considered.

2.2 Los Cinco Ojos aqueduct

Los Cinco Ojos aqueduct (Fig. 2(a)) is an eighteenth-century monument located near Alicante, in Spain. It is a 46.9 m long and 16.8 m high masonry structure with five arches

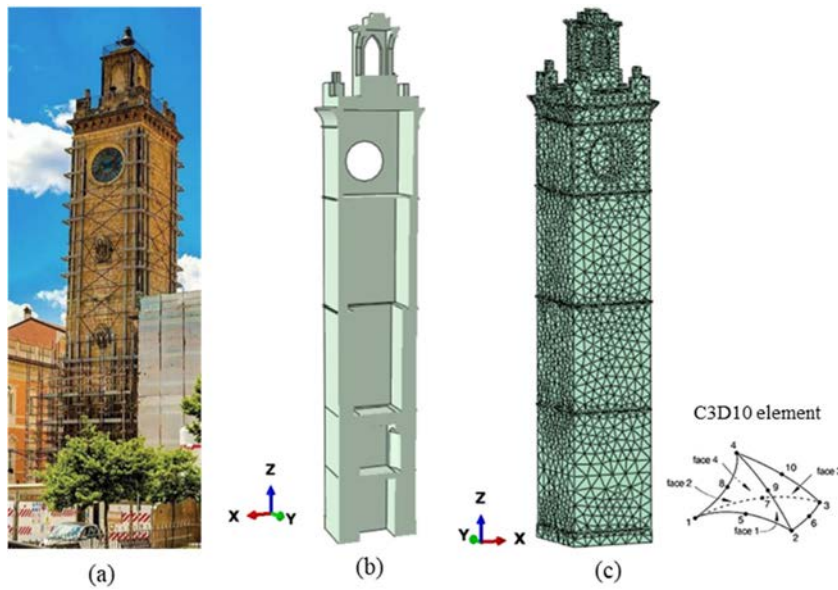

Figure 1: (a) L'Aquila civic tower; (b) Geometric; and (c) Numerical model.

Table 1: Identified masonry elastic homogeneous properties of the three models.

Numerical model	E (MPa)	G (MPa)	ρ (kg/m^3)
L'Aquila tower	3,286.50	1,264.00	1,900.00
Los Cinco Ojos aqueduct (brick masonry)	2,650.00	1,104.00	1,800.00
Los Cinco Ojos aqueduct (stone masonry)	1,350.00	563.00	1,400.00
Beit-el-Din hammam	1,400.00	637.00	1,800.00

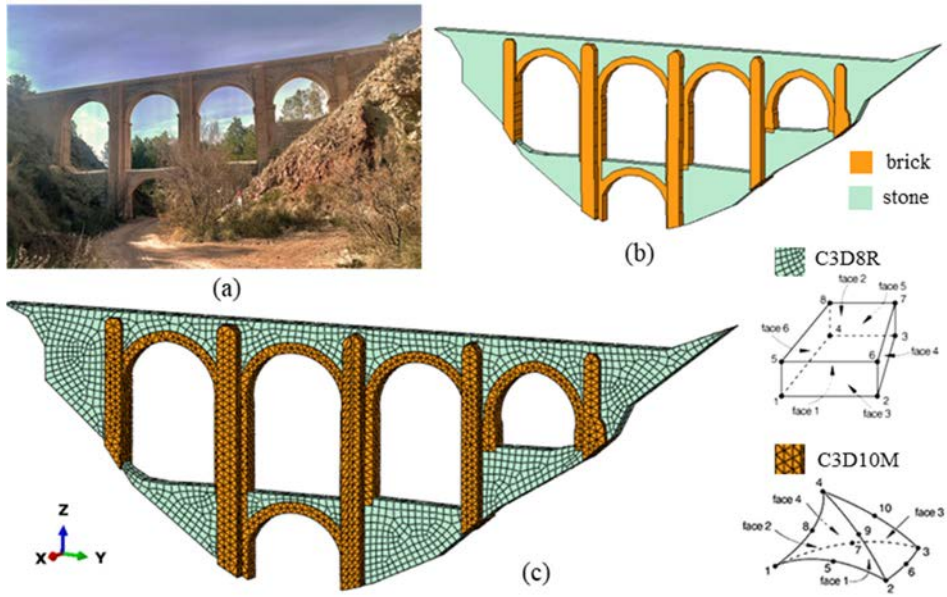

Figure 2: (a) Los Cinco Ojos aqueduct; (b) Geometric model; and (c) Numerical model.

(*ojos*) over two levels. It is made of two kinds of masonry: bricks (used for arches and piers) and stone (used for the other filling parts), see Fig. 2(b). On average, stone masonry and brick masonry are 1.10 m and 2.71 m thick, respectively. A numerical model of the aqueduct was built and identified with experimental frequencies in ABAQUS [9], by considering respectively C3D8R and C3D10M elements for stone and brick masonry (Fig. 2(c)). The identified elastic parameters are provided in Table 1. Fix constraints along the lateral soil-abutments were assumed in the model.

2.3 The Beit-el-Din hammam

The hammam of Beit-el-Din is a stunning Lebanese monument built in the eighteenth-century and characterised by barrel-vaults and domes pierced by holes (Figs 3(a) and 3(b)). It is made of two masonry buildings, the highest of them being 7.5 m high (at the top of the dome) and having almost square base with about 10 m on each side. The seismic behaviour of the Beit-el-Din hammam was investigated in Gerges et al. [8], where a 3D numerical model (Fig. 3(c)) was built with C3D10 elements and identified through the first experimental frequencies (the identified parameters are given in Table 1). Fixed base constraints were assumed.

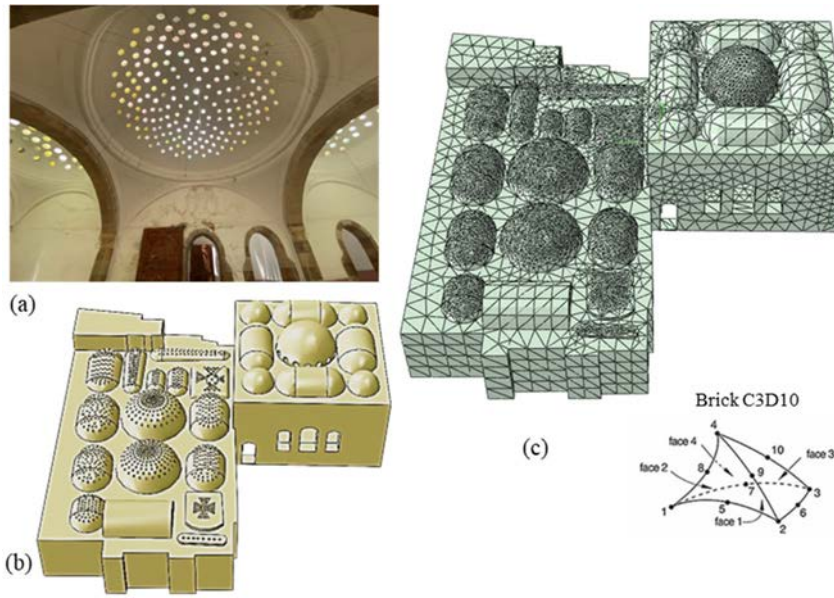

Figure 3: (a) Beit-el-Din hammam; (b) Geometric model; and (c) Numerical model.

3 NON-LINEAR DYNAMIC SEISMIC INVESTIGATION

Non-linear time-history (NLTH) analyses were carried out to assess the seismic performance of the three considered structures (tower, aqueduct and hammam) under different earthquakes. NLTH analyses typically involve the choice of parameters that are crucial to the results. Among them are the kind of spectrum-consistent earthquake considered in the analysis and the non-linear stress–strain law adopted for masonry. The concrete damage plasticity (CDP) law, with different tensile and compressive behaviour, has been adopted here for the considered structural models. The general tensile and compressive linearized curves are provided in Fig. 4. Details on the use of this model for historical masonry buildings can be found in Porcu et al. [2] and Gerges et al. [8]. The values of the CDP parameters assumed in the present investigation are given in Table 2. The ABAQUS default values have been set for the flow potential eccentricity, the shape factor K_c and the ratio between compressive yield stress in biaxial (f_{b0}) and uniaxial (f_{c0}), in agreement to the literature. As is usually done for existing structures, the dilatation angle (ratio between volume strain and shear strain) was set to 10°. The CDP linearized diagrams of Fig. 4 were derived for the three structures and the four materials considered. Initially, the tensile strength was assumed to be 1/30 of the compressive strength, which means assuming a strength ratio $Rs = \frac{\sigma_{t,A}}{\sigma_{c,A}} = 1/30$. Table 3 provides the values adopted for the different masonry structures, under the assumption of Rs = 1/30. In Section 4.3, different strength ratios are considered to assess the influence of this parameter.

3.1 Response spectra and considered spectrum-consistent earthquakes

The horizontal elastic response spectra provided by Italian, Lebanese [10] and Spanish codes respectively for L'Aquila, Beit-el-Din and Alicante are plotted together in Fig. 5. They refer

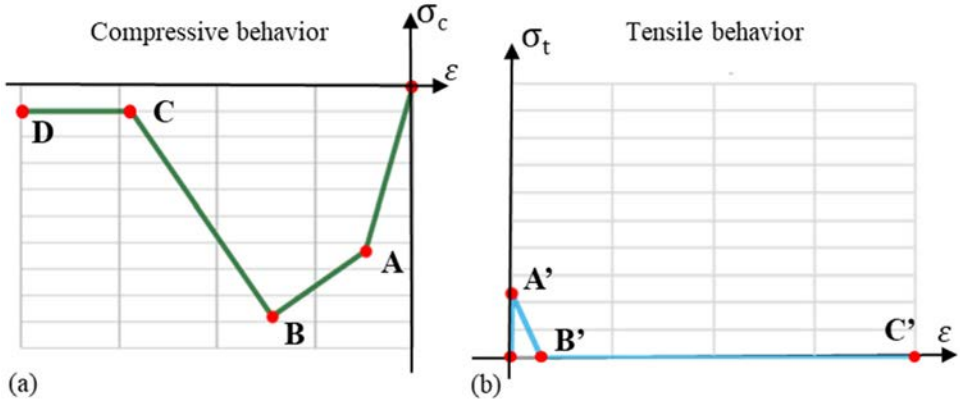

Figure 4: (a) Compressive and (b) tensile uniaxial stress–strain curves for the CDP model.

Table 2: CDP model: assumed parameters' values in ABAQUS.

Dilatation angle	Eccentricity	f_{b0}/f_{c0}	K_c	Viscosity
10°	0.1	1.16	0.667	5.00E-05

Table 3: Assumed values for compressive and tensile stress–strain curves (*Rs* = 1/30).

Compression (negative values)								
Model	$\sigma_{c,A}$ **(MPa)**	$\varepsilon_{c,A}$ **(%)**	$\sigma_{c,B}$ **(MPa)**	$\varepsilon_{c,B}$ **(%)**	$\sigma_{c,C}$ **(MPa)**	$\varepsilon_{c,C}$ **(%)**	$\sigma_{c,D}$ **(MPa)**	$\varepsilon_{c,D}$ **(%)**
Tower	6.00	0.0018	8.00	0.0054	1.00	0.0108	1.00	0.10
Aqueduct (brick)	6.30	0.0024	8.82	0.0072	1.00	0.0144	1.00	0.10
Aqueduct (stone)	2.30	0.0017	3.22	0.0052	0.365	0.0105	0.30	0.10
Hammam	2.00	0.143	3.20	0.4	0.35	0.50	0.35	0.60
Tension (positive values)								
Numerical model	$\sigma_{t,A}$ **(MPa)**	$\varepsilon_{t,A}$ **(%)**	$\sigma_{t,B}$ **(MPa)**	$\varepsilon_{t,B}$ **(%)**	$\sigma_{t,C}$ **(MPa)**	$\varepsilon_{t,C}$ **(%)**		
Tower	0.2	0.0001825	0.0005	0.002182	0.0005	0.10		
Aqueduct (brick)	0.21	0.00008	0.0005	0.00208	0.0005	0.10		
Aqueduct (stone)	0.076667	0.00006	0.0002	0.00148	0.0002	0.10		
Hammam	0.066	0.00476	0.0033	0.15	0.0033	0.15		

to soil Type III/C and life protection limit state. The effect of the vertical component is not assessed in this study. The Lebanese spectrum is obtained according to American IBC [11] as allowed by Lebanese code [10] (see Gerges et al. [12] for details). It is worth noting that Beit-el-Din and L'Aquila code spectra are rather similar, while the Alicante spectrum has

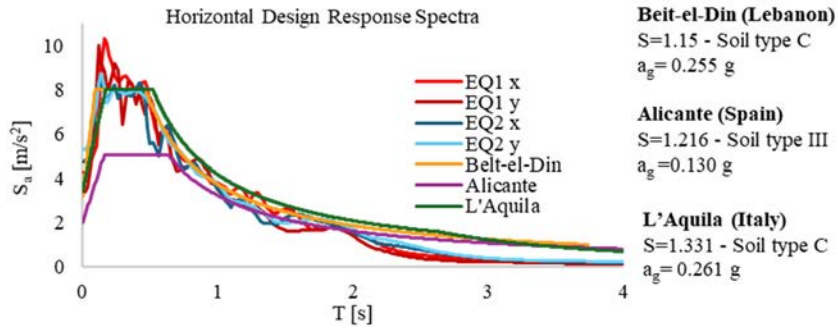

Figure 5: Code-based horizontal elastic response spectra and earthquake response spectra.

lower accelerations, due to the minor seismicity of the Spanish area. To obtain spectrum-consistent earthquakes, reference to the Beit-el-Din spectrum was made, since it is very close to the L'Aquila one and higher than the Alicante spectrum. Consistent with the Beit-el-Din code response spectrum, two earthquakes were thus obtained and referred to as EQ1 and EQ2, see Table 4 and Fig. 6. Roughly, EQ1 and EQ2 can be taken as a multi-peak and a pulse-like earthquake, respectively. Based on the Arias intensity [13], the procedure shown in Gerges et al. [12] was applied to obtain shorth-length accelerograms with 90% of the earthquake energy (red box in the figure) to reduce computational burden in the numerical analyses.

Table 4: Characteristics of the considered earthquakes.

Earthquake	Event ID	Station	Date	Magnitude	Epicentre (km)
EQ1	EMSC.20180704_	Dead Sea/Jourdan	2018/04/07	4.1	159
EQ2	IL-1987-0002	Dead Sea/Izrael	1984/08/24	5.3	34.8

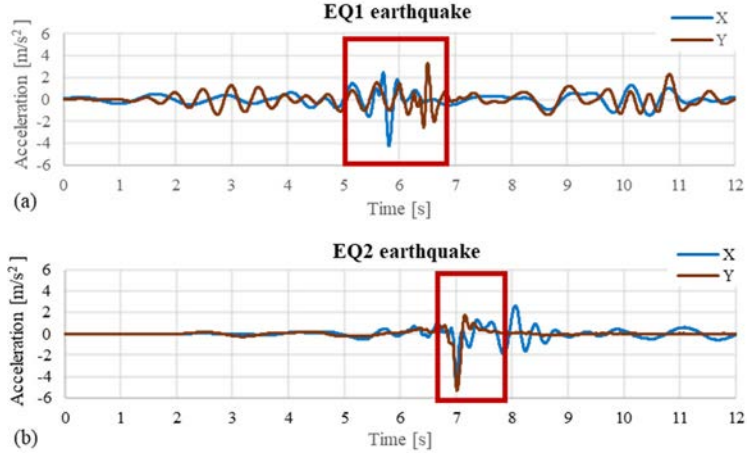

Figure 6: (a) Multi-peak EQ1 earthquake; and (b) Pulse-like EQ2 earthquake. Red windows indicate the short length accelerograms used in the analysis.

4 NUMERICAL INVESTIGATION

A numerical investigation was performed to assess the role of the structural shape, of the earthquake type, and of the strength ratio.

4.1 Role of the structural shape (tower-like, multi-arched and multi-vaulted structures)

Figs 7 and 8 provide the contours of the maximum principal plastic strain (PE) in the three structures, taken at the end of the numerical simulation under EQ1 and EQ2. Dark red indicates tensile plastic strain. It can be noted that the three structures are differently affected by the same earthquake, due to their dissimilar geometric shape and dynamical behaviour. In the tower, the vertical edges are the most affected structural parts where typically cracks initiate. The zones around the circular hole are affected by local concentration of stress, which do not generally cause threatening damage. In the aqueduct, the highest inelastic tensile demand occurs along the abutments and in the spandrel regions between upper arches and vertical elements. These regions correspond to contact areas where materials of differing stiffness (weaker stone masonry and stiffer brick masonry) meet, and the thrust of the arches is concentrated or transferred into the supporting elements, leading to stress concentrations and potential cracking. On the other hand, arches and vaults are the most affected structural elements in the hammam, where three hinges are developed in some dome sections. It is to stress, however, that four hinges imply the collapse of an arch.

4.2 Role of the earthquake type

It is well known that the earthquake demand on structures is strictly related to the characteristics of the ground motion, although the geometric and dynamic characteristics of the structures are recognized to play a key role too [14]. The comparisons in Figs 7 and 8 illustrate the differing responses of the three structures under the two considered earthquakes.

EQ2 produces larger tensile damage either in the tower and the aqueduct, while EQ1 is the most damaging to the hammam. Figs 9 and 10 help explain why the two earthquakes pose different levels of threat to the three structures. External total work on the three structures under EQ1 and EQ2 is plotted in Figs 9(a) and 10(a), while the corresponding inelastic dissipated energy is plotted in Figs 9(b) and 10(b). In all the considered cases the external work is quasi-one-order of magnitude higher than the dissipated energy. This is a typical behaviour of masonry, where a large amount of energy is dissipated by means of elastic mechanisms (rocking or sliding) and/or opening and closing of cracks, without permanent plastic deformation. Figs 9(a) and 10(a) show that the maximum external work involved by EQ2 is up to almost 250,000 J for the aqueduct and more than 150,000 for the tower. In both cases it is notably higher than that involved under EQ1 (less than 100,000 J). Accordingly, for the tower and the aqueduct, the inelastic dissipated energy and thus the damage is larger under EQ2 than under EQ1. On the contrary, for the hammam, external work and dissipated energy are slightly higher under EQ1 than under EQ2, although the difference between the EQ1 and EQ2 demand is less marked in this case.

4.3 Role of strength ratio *Rs*

Unreinforced masonry is a heterogeneous material with distinct anisotropic behaviour under tension and compression. Resistance to tension is characteristically very low, so values of strength ration *Rs* ranging from 1/10 to 1/60 are adopted in literature when modelling the

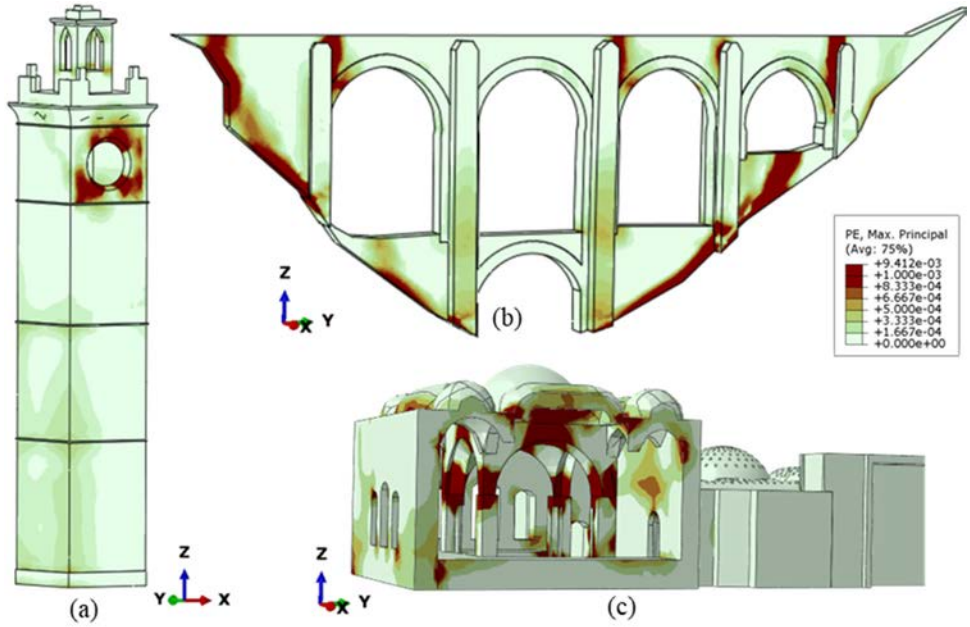

Figure 7: Damage pattern due to tensile strain under EQ1 for (a) the tower; (b) the aqueduct; and (c) the hammam (*Rs* = 1/30).

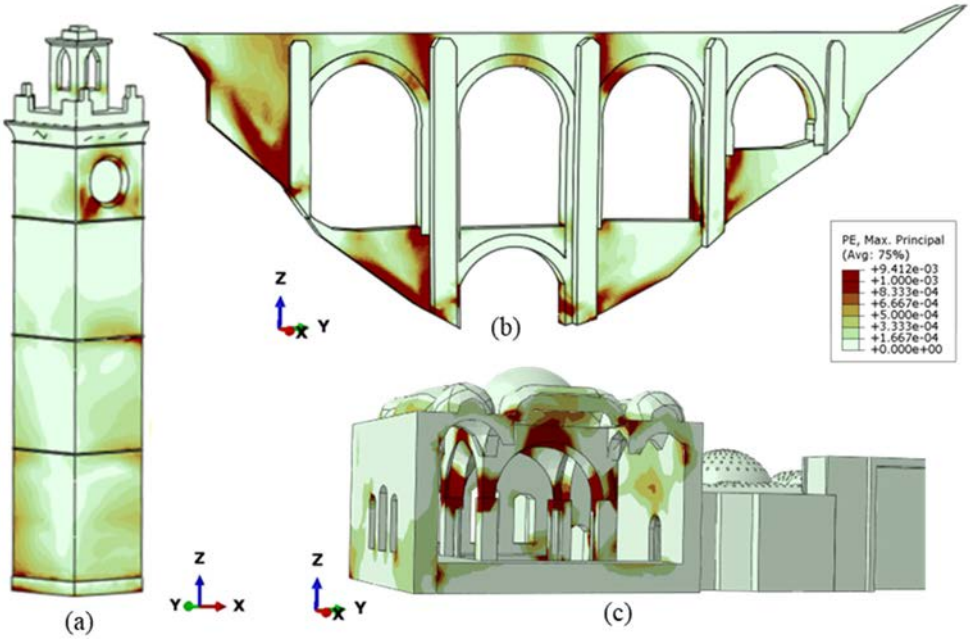

Figure 8: Damage pattern due to tensile strain under EQ2 for (a) the tower; (b) the aqueduct; and (c) the hammam (*Rs* = 1/30).

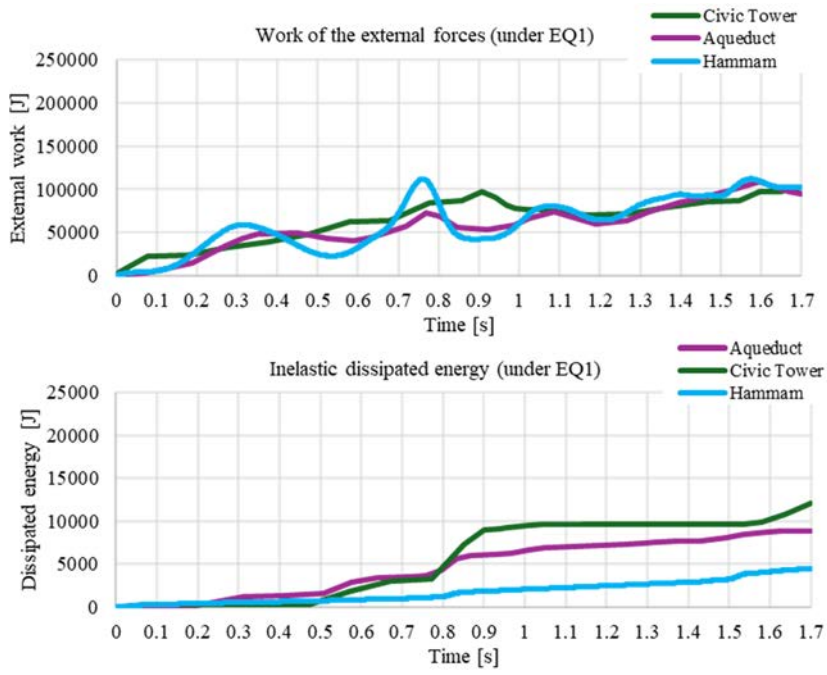

Figure 9: (a) External work; and (b) Inelastic energy dissipated under EQ1.

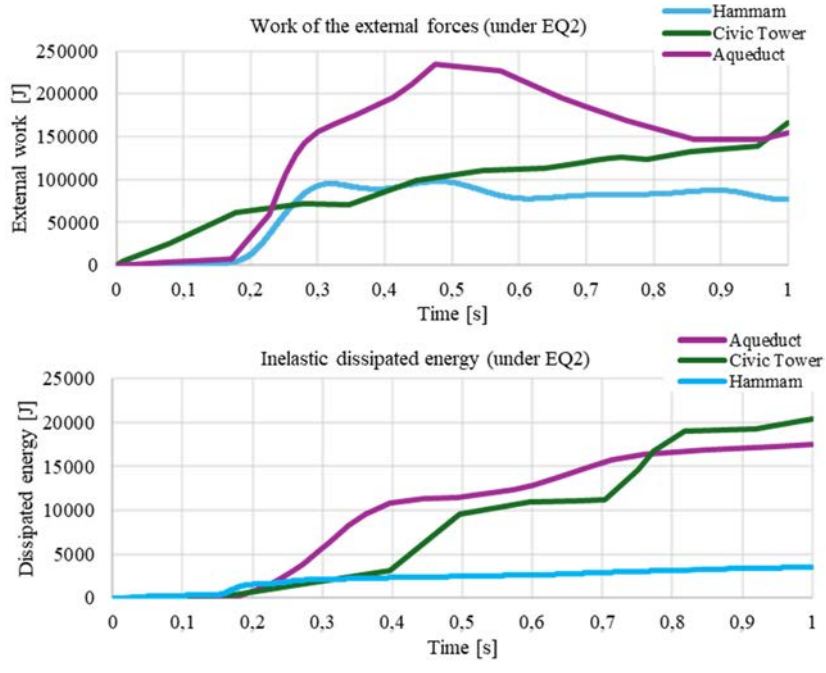

Figure 10: (a) External work; and (b) Inelastic energy dissipated under EQ2.

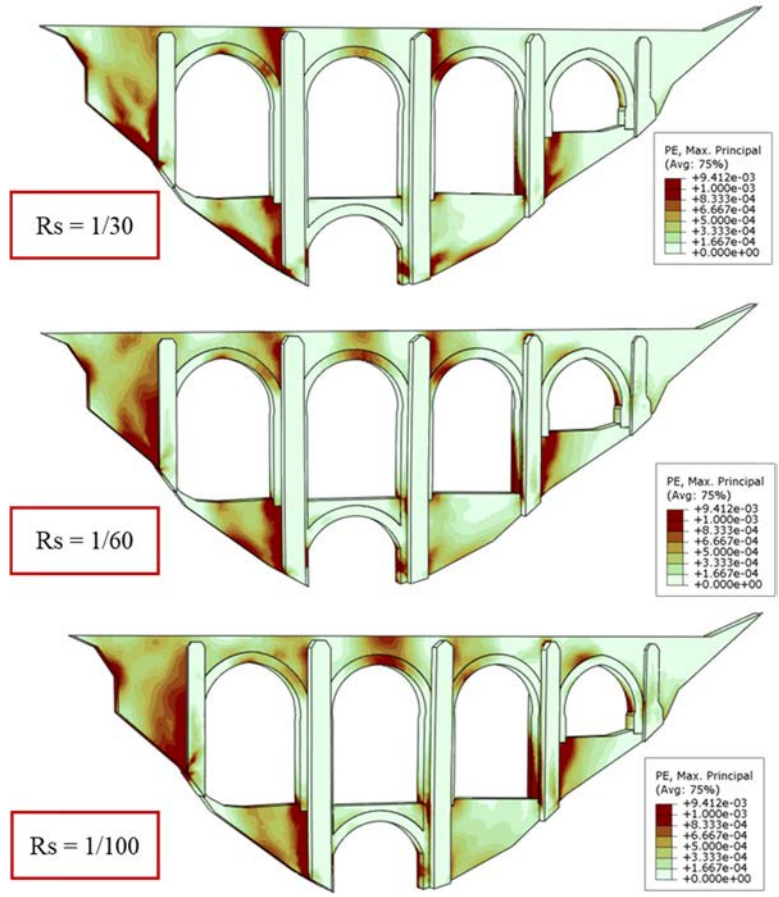

Figure 11: Los Cinco Ojos aqueduct: influence of the strength ratio *Rs* (EQ2 earthquake).

masonry constitutive behaviour through the CDP law [2], [6], [8], [15]. Adopting higher or lower strength ratio affect results of the numerical analyses. Figs 11 and 12 show the plastic strain contours of the Los Cinco Ojos aqueduct for three different values of *Rs* under EQ2. Fig. 11 shows that the spread of damage increases as *Rs* decreases, while a plastic hinge develops at the keystone of the upper central arch. It is worth noting that the collapse mechanism due to the formation of four hinges in one of the aqueduct's arches is rather unlikely, as can be inferred by the present results. The out-of-plane collapse mechanism can be more dangerous for the aqueduct. Figs 12(a) and 12(b) show the out-of-plane top displacements of the aqueduct under the two earthquakes, for the three different values of *Rs*. Almost 12 cm are reached under EQ2 for *Rs* = 1/100.

5 CONCLUSIONS

The paper presents a numerical comparison of the seismic post-elastic performance of three historical masonry structures taken as representative of different structural behaviour: a tower, a multi-arched aqueduct, and a multi-vaulted hammam. The research focused on

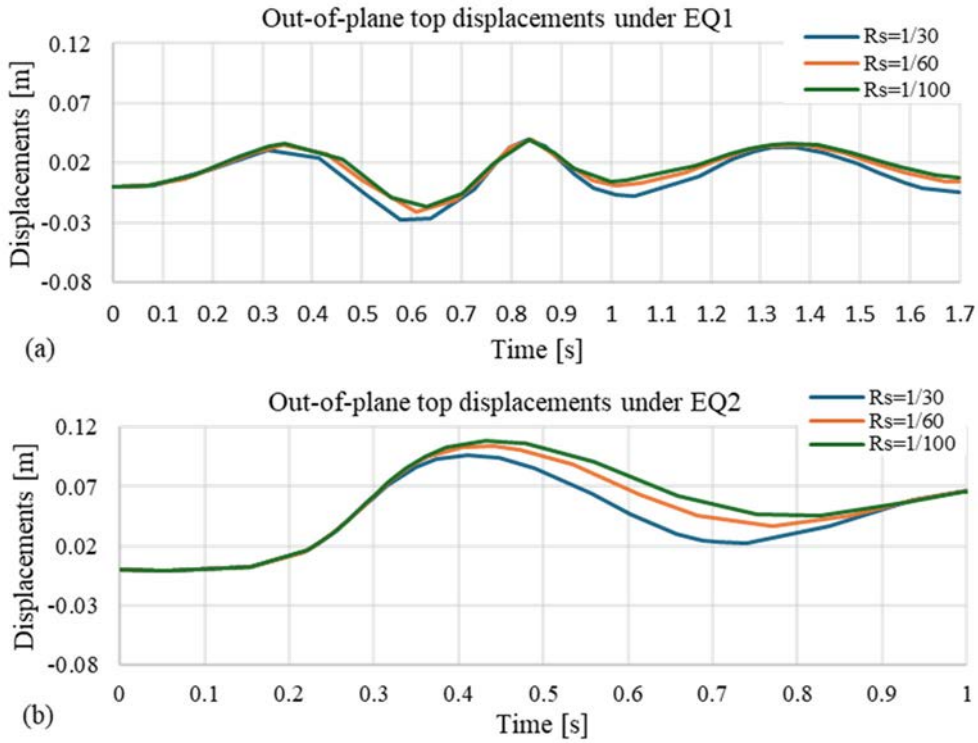

Figure 12: Top displacements of the aqueduct under EQ1 (a) and EQ2 (b) for different *Rs*.

assessing the influence of structural geometry, earthquake characteristics, and tensile-to-compressive strength ratio on seismic response. The results highlight the critical role of structural shape in seismic performance. The tower exhibited stress concentrations at its corners, which are common locations for fracture initiation. The aqueduct was affected by significant inelastic tensile demand at the abutments and spandrel regions rather than in the arches, indicating that the dominant failure mechanism is out-of-plane. The hammam was most vulnerable at the arches beneath the main dome, where the formation of a sufficient number of hinges could potentially lead to collapse. Earthquake type significantly influenced the structural response too. The pulse-like EQ2 caused greater damage to the tower and aqueduct, while the multi-peak EQ1 was more detrimental to the hammam. Furthermore, lower tensile-to-compressive strength ratio *Rs* led to greater damage propagation, as seen in the aqueduct, which experienced out-of-plane displacements of up to 12 cm under EQ2 for *Rs* = 1/100. This study confirms that different structural typologies exhibit distinct failure mechanisms under seismic loading, underscoring the need for structure-specific seismic assessments of historical masonry buildings.

ACKNOWLEDGEMENTS

It is acknowledged the financial support under the National Recovery and Resilience Plan (NRRP), Mission 4, Comp. 2, Investment 1.1, Call for tender No. 1409 published on 14.9.2022 by the Italian Ministry of University and Research (MUR), funded by the European Union – NextGenerationEU–CUP F53D23009640001 – Assignment Decree n. P20227CSJ5.

REFERENCES

[1] Scamardo, M., Zucca, M., Crespi, P., Longarini, N. & Cattaneo, S., Seismic vulnerability evaluation of a historical masonry tower: Comparison between different approaches. *Applied Sciences*, **12**(21), 11254, 2022. https://doi.org/10.3390/app122111254.

[2] Porcu, M.C., Montis, E. & Saba, M., Role of model identification and analysis method in the seismic assessment of historical masonry towers. *Journal of Building Engineering*, **43**, 103114, 2021. https://doi.org/10.1016/j.jobe.2021.103114.

[3] Ivorra, S., Baeza, F.J., Bru, D. & Varona, F.B., Seismic behavior of a masonry chimney with severe cracking condition: Preliminary study. *KEM*, **628**, pp. 117–122, 2014. https://doi.org/10.4028/www.scientific.net/KEM.628.117.

[4] Ivorra, S., Pallarés, F.J. & Adam, J.M., Experimental and numerical results from the seismic study of a masonry bell tower. *Advances in Structural Engineering*, **12**(2), pp. 287–293, 2009. https://doi.org/10.1260/136943309788251641.

[5] Addessi, D., Liberatore, D. & Nocera, M., Damaging behavior of masonry arch bridges: Analysis of 'Ponte delle Torri' in Spoleto, Italy. *Journal of Earthquake Engineering*, **26**(1), pp. 449–474, 2022. https://doi.org/10.1080/13632469.2019.1690599.

[6] Bertolesi, E., Milani, G., Lopane, F.D. & Acito, M., Augustus Bridge in Narni (Italy): Seismic vulnerability assessment of the still standing part, possible causes of collapse, and importance of the Roman concrete infill in the seismic-resistant behavior. *International Journal of Architectural Heritage*, pp. 1–30, 2017. https://doi.org/10.1080/15583058.2017.1300712.

[7] Zucca, M., Reccia, E., Vecchi, E., Pintus, V., Dessì, A. & Cazzani, A., An evaluation of the structural behaviour of historic buildings under seismic action: A multidisciplinary approach using two case studies. *Applied Sciences*, **14**(22), 10274, 2024. https://doi.org/10.3390/app142210274.

[8] Gerges, A., Porcu, M.C. & Cazzani, A., Numerical investigation of the post-elastic seismic response of the multi-vaulted Beit-El-Din Hammam. *IJMRI*, **9**(5–6), pp. 537–566, 2024. https://doi.org/10.1504/IJMRI.2023.10058266.

[9] ABAQUS, *Theory Manual*, 2023.

[10] Ministry of Industry. The Lebanese Standards Institution (LIBNOR), *NL:135*, Beirut, Lebanon, 2012.

[11] IBC, Ch.16 S.13 Earthquake loads. *International Building Code*. International Code Council: Washington, DC, USA,.

[12] Gerges, A., Porcu, M.C. & Vielma Pérez, J.C., A contribution to facilitate the seismic design in Lebanon using short-length spectrum-consistent earthquakes. *Applied Sciences*, **13**(24), 12990, 2023. https://doi.org/10.3390/app132412990.

[13] Arias, A., A Measure of earthquake intensity. *Seismic Design for Nuclear Power Plants*, ed. R.J. Hansen, MIT Press: Cambridge, MA, USA, 1970.

[14] Gümüş, M. & Durucan, C., Effects of pulse like ground motion records with and without acceleration pulses on the earthquake responses of structures with varying dynamic properties. *Structures*, **45**, pp. 427–436, 2022. https://doi.org/10.1016/j.istruc.2022.09.042.

[15] Valente, M. & Milani, G., Seismic assessment of historical masonry towers by means of simplified approaches and standard FEM. *Construction and Building Materials*, **108**, pp. 74–104, 2016. https://doi.org/10.1016/j.conbuildmat.2016.01.025.